Article

Pharmacoinformatics and molecular docking simulation-based phytochemical screening of *Artocarpus altilis* against SARS-CoV-2 by targeting M^pro

Md Afif Ullah[1], Md Mehedy Hasan Miraz[1], Nilay Saha[1], Arghya Prosun Sarkar[2], Bidduth Kumar Sarkar[3] and Sukalyan Kumar Kundu[1,*]

Abstract

A sudden onset of an emergent viral pathogen, SARS-CoV-2, manifested globally in late December 2019, originating in Wuhan, China, swiftly precipitating the COVID-19 pandemic. Subsequent to its rapid dissemination, intensive research efforts have been dedicated to identifying effective therapeutic modalities to counteract this formidable virus. In this context, a computational scrutiny of compounds derived from *Artocarpus altilis* (breadfruit) was undertaken to discern potential inhibitors of the SARS-CoV-2 main protease (M^pro) enzyme, crucial for viral replication. Initiating our investigation, a comprehensive drug-likeness analysis was employed to discern compounds with optimal pharmacological attributes. Subsequently, molecular docking studies were conducted, focusing on the Mpro enzyme, with selected compounds from *A. altilis*. Nirmatrelvir, an FDA-approved drug in combination with ritonavir, served as the benchmark inhibitor in these analyses. The compounds under investigation, namely cycloartomunin, dihydrocycloartomunin, cycloartobiloxanthone, artomunoxanthentrione, and cycloartomunoxanthone demonstrated notable binding affinities of -7.6, -7.7, -7.7, -8.3, and -8.1 kcal/mol, respectively, in the molecular docking studies. Comparative analysis revealed nirmatrelvir to exhibit an affinity of -8.1 kcal/mol in the same docking environment. Subsequently, a comprehensive pharmacological assessment was undertaken, juxtaposing the top five test compounds with the standard inhibitor. Concomitant with this, a computational toxicity analysis was integral to our assessment. Ultimately, the investigated compounds displayed promising docking outputs coupled with moderate pharmacological profiles. This study advocates further experimental validations to ascertain the inhibitory potential of these *A. altilis*-derived compounds against the SARS-CoV-2 M^pro enzyme.

Keywords: COVID-19, SARS-CoV-2, M^pro enzyme, breadfruit, *Artocarpus altilis*, molecular docking.

[1]Department of Pharmacy, Jahangirnagar University, Savar, Dhaka-1342, Bangladesh; [2]Department of Pharmacy, Faculty of Biological Sciences, Islamic University, Kushtia, Bangladesh; [3]Department of Pharmacy, Faculty of Science, Comilla University, Comilla

* Correspondence: Prof. Dr. Sukalyan Kumar Kundu, Department of Pharmacy, Jahangirnagar University, Savar, Dhaka, Bangladesh; Email: skkbd415@juniv.edu, Phone: +8801731291468

Introduction

The SARS-CoV-2 outbreak in late 2019 and its global propagation have had substantial global consequences on public health, economics, and social aspects (Miyah et al., 2022). SARS-CoV-2, also known as COVID-19, is a highly pathogenic virus that was discovered in Wuhan, China, near the end of 2019 (Hu et al., 2021; Ludwig & Zarbock, 2020). Since then, it has swiftly spread over the world, and the World Health Organization (WHO) designated it a global pandemic in March 2020 (Patnaik, 2021). As a result of the pandemic, many countries throughout the world imposed tight measures such as lockdowns and travel restrictions to prevent the spread of COVID-19 (Inoue & Todo, 2020; Zhong et al., 2021). Until November 22, 2023, the World Health Organization (WHO) had recorded over 772 million COVID-19 cases globally (https://covid19.who.int/). Regrettably, the aforementioned has led to a total of more than 6.98 million fatalities, which is a substantial figure in comparison to other diseases (WHO, 2023).

The causative agent of COVID-19, SARS-CoV-2, is a positive-sense, single-stranded RNA virus belonging to the family of Coronaviridae (Hu et al., 2020). The virus's surface has a special spike protein that binds to the human angiotensin-converting enzyme 2 (ACE2) receptor. This makes it easier for the virus to get into host cells and start copying itself (Deng et al., 2021). The SARS-CoV-2 virus has undergone significant mutations, leading to the emergence of several new variants (WHO, 2022).

The main protease (Mpro) enzyme in SARS-CoV-2 is very important for the virus to replicate and is thought to be a good target for drugs that could help treat COVID-19 (Huynh et al., 2021). M^{pro}, also known as 3CL pro, is responsible for the proteolytic cleavage of the viral polypeptide during replication, which is essential for the production of functional viral proteins(Dharmashekara et al., 2021).The inhibition of M^{pro} can potentially prevent viral replication and transmission, making it a valuable target for drug development against COVID-19 (Citarella et al., 2021).Recent years have seen a lot of research into the structure and function of Mpro. This has led to the creation of a number of inhibitors that target this protease (Hu et al., 2022). These inhibitors have shown effective inhibition of M^{pro} in vitro and in vivo, demonstrating their potential as a therapeutic option for treating COVID-19 (Li et al., 2021).

Artocarpus altilis, commonly referred to as breadfruit, belongs to the family Moraceae (Turi et al., 2015). It is a notable plant with a substantial therapeutic profile (Sikarwar et al., 2014). Many ongoing studies are looking at the pharmacological effects of *Artocarpus altilis*. Anti-inflammatory activity, antioxidant activity, antimicrobial potential, immunomodulatory potential, anti-diabetic activity, anti-cholinergic effect, chelating activity, nutritional assessment, as a cosmetic agent, ACE inhibitors, and other studies are being conducted on these plants (Ajiboye et al., 2020; Jalal et al., 2015; Riasari et al., 2019; Tara Kamal, 2012). Surprisingly, the activity of this plant against SARS-CoV-2was previously undocumented in the literature. As a result, it was chosen for this investigation to investigate its action against the targets of Omicron variant SARS-CoV-2.

Nirmatrelvir–ritonavir (Paxlovid™), which has received emergency use authorization by the Food and Drug Administration (FDA) for the outpatient treatment of COVID-19 infection in adults (Gui et al., 2023). Nirmatrelvir is a SARS-CoV-2 M^{pro} inhibitor, which actively inhibits the viral replication process by blocking the virus from cleaving viral polyproteins into their functional parts, thus limiting the infection's spread in the body (Park et al., 2022). Multiple studies have shown that nirmatrelvir–ritonavir has potent inhibitory activity against SARS-CoV-2 proteases, making it a promising candidate for COVID-19 treatment (Rodrigues et al., 2022). A clinical trial by Pfizer, the developer of nirmatrelvir/ritonavir, reported that nirmatrelvir/ritonavir treatment reduced the risk of hospitalization or death by 89% in patients with mild to moderate COVID-19 symptoms (Huang et al., 2022). Thus, we have considered nirmatrelvir as a standard inhibitor in our assessment.

Computer-aided drug design (CADD) is a computational method that uses various software tools and algorithms to create, optimize, and test new drugs before they can be synthesized and tested in the lab (Yu & MacKerell, 2017). In this computational assessment, we implemented molecular docking, pharmacokinetic and pharmacodynamic property studies to discover the best possible drug candidate. Molecular docking provided us with information on each ligand's binding affinity, direction, and kind of interaction with the appropriate target proteins. The pharmacokinetic profiles were obtained in order to analyze data on the absorption, distribution, metabolism, and excretion (ADME) of chemicals that occur inside the body following medication delivery. To determine the LD50 values and toxicity classes of the various ligands, a toxicology scrutiny was conducted.

In the current work, we used a screening method to filter out 10 phytochemical compounds from *A. altilis* based on drug-likeness criteria. Through preliminary computational analysis, the compounds were examined across a wide spectrum of studies. As a result, this

framework evaluates and offers potential promising *A. altilis* medication candidates against the SARSCoV-2 Omicron B.1.1.529 strain.

Materials and Methods

Selection and Preparation of Ligands
A total of ten phytochemicals derived from *Artocarpus altilis* were chosen for this investigation based on their drug-likeness. The molecules were chosen using Lipinski's rule of five and the Ghose filter (Khan et al., 2019; Nogara et al., 2015). Only molecules that followed both rules were chosen for this investigation. The chosen ligands' 3D conformers were obtained in SDF format from the online databases PubChem (https://pubchem.ncbi.nlm.nih.gov/) and IMPPAT 2.0 (Indian Medicinal Plants, Phytochemistry, and Therapeutics; https://cb.imsc.res.in/imppat/) (Kim et al., 2016; Vivek-Ananth et al., 2023).

Retrieval and Preparation of Target Protein
The crystal structure of the M^{pro} enzyme (PDB ID: 8D4L) of SARS-CoV-2 was retrieved in PDB format from the RCSB Protein Data Bank database (https://www.rcsb.org/) (Dejnirattisai et al.,2022; Rose et al.,2016). The resolution of the downloaded spike protein was 1.70°A. The protein structures were cleaned by eliminating unwanted atoms and molecules (including ligands) with PyMOL version 2.5.2 software (Schrodinger, LLC) (Lill et al., 2011). The spike protein's receptor-binding domain (RBD) was taken out of the crystal structure, and PyMOL was used to get rid of the extra protein chains. The proteins' chains were stored in PDB formats for molecular docking (Morris & Lim-Wilby, 2008).

Molecular Docking
The CB-Dock2 server (https://cadd.labshare.cn/cb-dock2/php) was used to execute molecular dockings on the chosen ligands against the target proteins (Liu et al., 2022). The binding affinity (kcal/mol) for each protein-ligand combination, as well as noncovalent interactions and docking orientations, were examined using the Dassault Systmes BIOVIA Discovery Studio 2021 Client version 21.1.0 software (Baroroh, S.Si., M.Biotek. et al., 2023). The 2D and 3D schematic drawings of the protein-ligand docking complexes were obtained from BIOVIA Discovery Studio (BIOVIA, Dassault Systèmes, 2023).

ADME and Toxicity Prediction
The top-docking ligands' canonical SMILES were taken from the PubChem and IMPPAT 2.0 databases and entered into the SwissADME website (https://www.swissadme.ch/) (Daina et al., 2017; Kim et al., 2019). SwissADME provided the ADME (absorption, distribution, metabolism, and excretion)

statistics for each ligand. Following that, the ProTox-II service (https://tox-new.charite.de/protox_II/) was used to estimate the toxicity profile of each ligand (Banerjee et al., 2018). These two sources were used to record the physicochemical, pharmacokinetic, and pharmacodynamic aspects of each ligand. During the ADME and toxicity prediction, each ligand's topological polar surface area (TPSA), lipophilicity (MLogP), water solubility (LogS), bioavailability score, blood-brain barrier (BBB) permeability, interaction with P-glycoprotein (P-gp), LD50 value, and toxicity class were explored.

Results and Discussion

The docking score, or binding affinity, of a ligand denotes the level of attraction at which the ligand is supposed to bind to the target (Figure 1) (Pantsar & Poso, 2018). The docking conformations show at which orientation the ligands bind to the respective targets (Figure 2). A complete docking operation includes the bond types, bond lengths, and a complete overview of the ligand's static interactions with the target (Guedes et al., 2014). Artomunoxanthentrione displayed the highest binding affinity, which is −8.3 kcal/mol. It was found to exhibit almost 20 interactions with the amino acid residues of M^{pro}. The interactions obtained from the CB-Dock2 server for each molecule have been mentioned in Table 1. The binding affinities of cycloartomunin, cihydrocycloartomunin, cycloartobiloxanthone, artomunoxanthentrione, cycloartomunoxanthone, and nirmatrelvir (standard) in complex were −7.6, −7.7, −7.7, −8.1, and −8.1 kcal/mol, respectively.
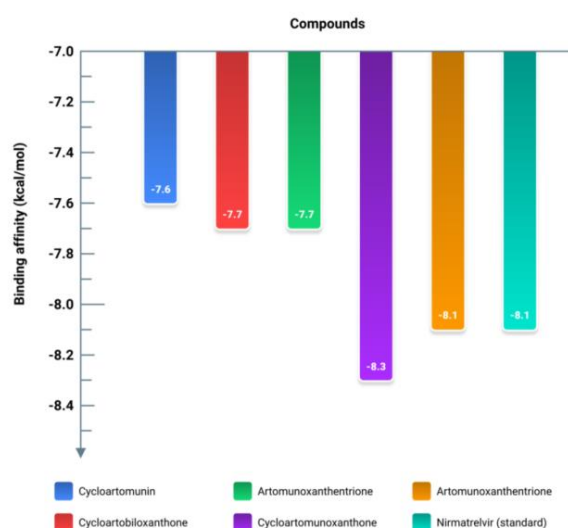

Figure 1: Binding affinity chart of each compound in complex with M^{pro} enzyme of SARS-CoV-2.

Table 1: The binding affinities and noncovalent (hydrogen bonds and hydrophobic) interactions of the test compounds and the standard inhibitor (nirmatrelvir).

Chemical ID (Source)	Compound Name	Binding affinity (kcal/mol)	Interactions
IMPHY000132 (IMPPAT)	Cycloartomunin	−7.6	GLN107 PRO108 GLY109 GLN110 PRO132 ILE200 VAL202 GLU240 PRO241 HIS246 ILE249 THR292 PRO293 PHE294
IMPHY000674 (IMPPAT)	Dihydrocycloartomunin	−7.7	THR24 THR25 THR26 LEU27 HIS41 CYS44 THR45 SER46 MET49 PHE140 LEU141 ASN142 GLY143 ALA144 CYS145 HIS163 HIS164 GLU166 HIS172 GLN189
IMPHY001232 (IMPPAT)	Cycloartobiloxanthone	−7.7	HIS41 MET49 LEU141 ASN142 GLY143 CYS145 HIS163 HIS164 MET165 GLU166 LEU167 PRO168 GLN189
IMPHY001629 (IMPPAT)	Artomunoxanthentrione	−8.3	THR24 THR25 THR26 LEU27 HIS41 CYS44 THR45 SER46 MET49 PHE140 LEU141 ASN142 GLY143 ALA144 CYS145 HIS163 GLU166 LEU167 PRO168 GLN189
IMPHY001678 (IMPPAT)	Cycloartomunoxanthone	−8.1	THR24 THR25 THR26 HIS41 CYS44 THR45 SER46 MET49 PHE140 LEU141 ASN142 GLY143 ALA144 CYS145 HIS163 HIS164 MET165 GLU166 HIS172 GLN189
155903259 (PubChem)	Nirmatrelvir	−8.1	THR25 THR26 LEU27 HIS41 CYS44 THR45 SER46 MET49 PHE140 LEU141 ASN142 GLY143 ALA144 CYS145 HIS163 HIS164 MET165 GLU166 ARG188 GLN189
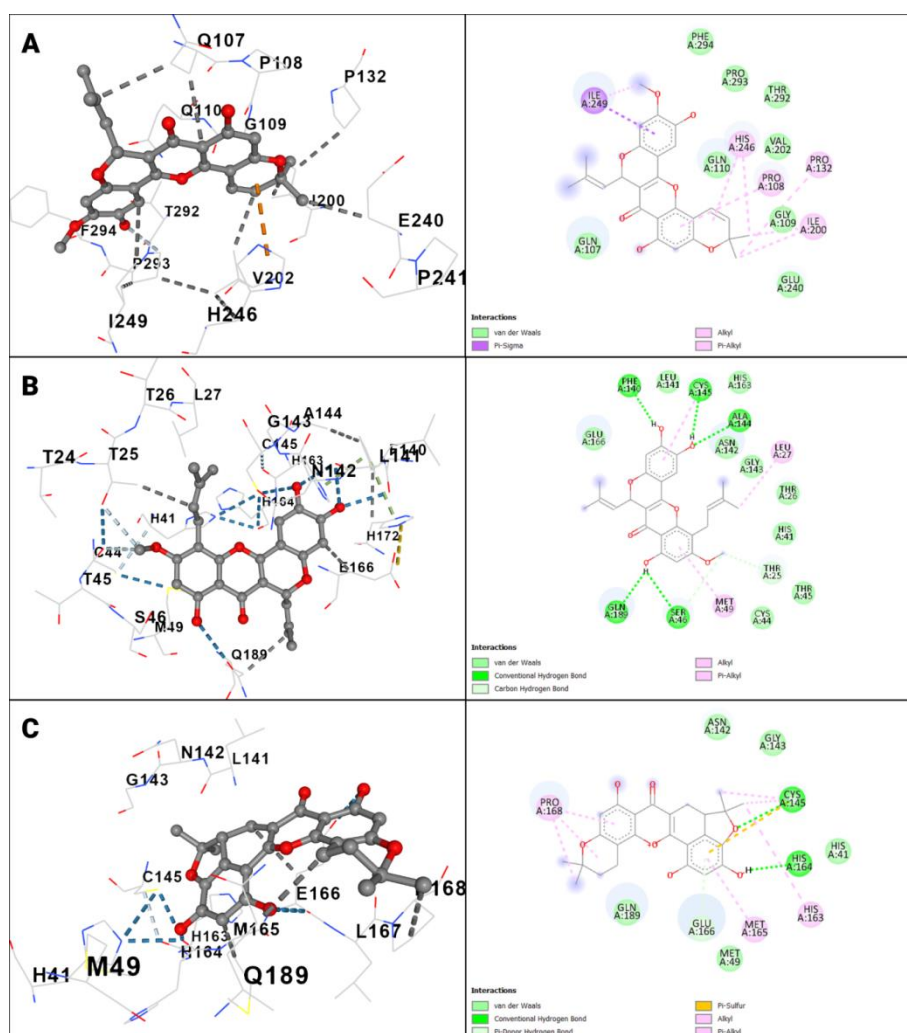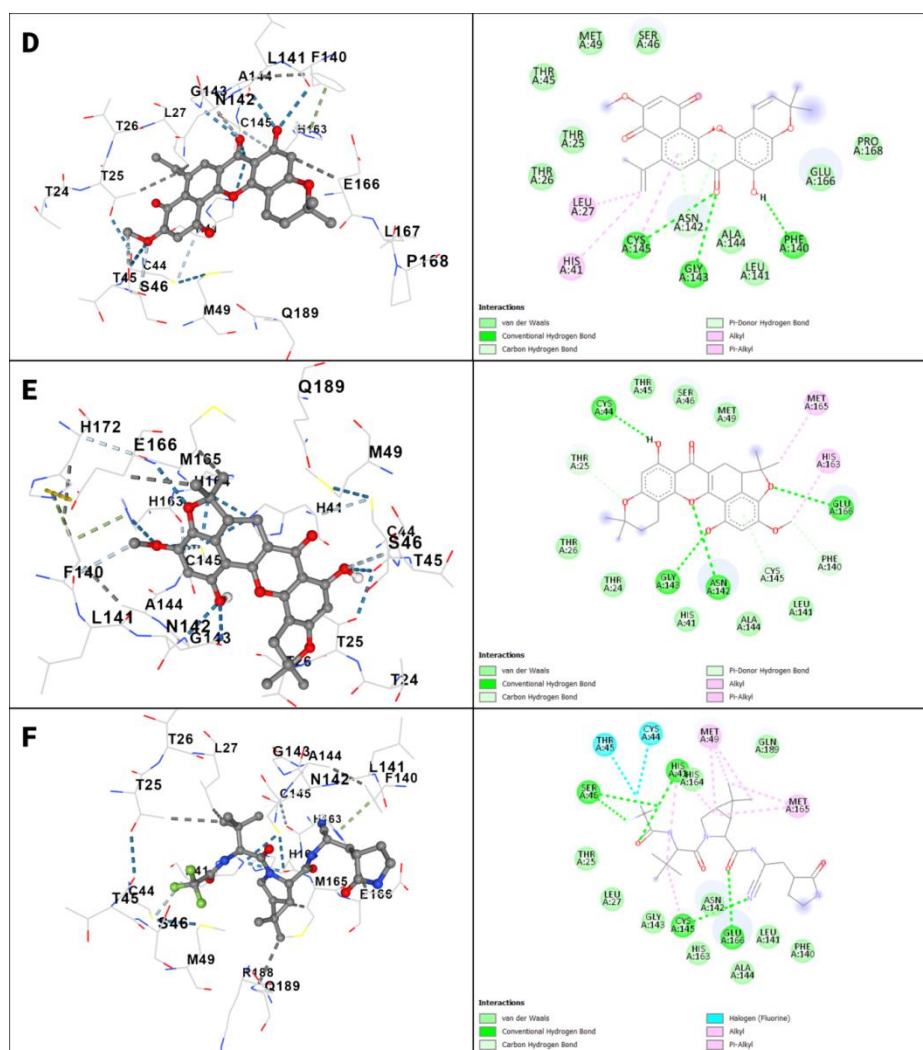
Figure 2: 3D conformations (left) and 2D view of the docking outputs of (A) cycloartomunin, (B) dihydrocycloartomunin, (C) cycloartobiloxanthone, (D) artomunoxanthentrione, (E) cycloartomunoxanthone, and (F) nirmatrelvir in complex with M^{pro}.

The physicochemical, pharmacokinetic, and pharmacodynamic aspects of the compounds were analyzed using the data obtained from Protox-II and SwissADME. The ADME profiles give a detailed overview of the molecular weights (MWs), topological polar surface areas (TPSAs), lipophilicity, water solubility, gastrointestinal absorptions, bioavailability scores, blood-brain barrier (BBB) permeability, and certain parameters for the ligands. These factors reflect how well molecules will be absorbed, distributed, metabolized, and eventually eliminated once they reach the human body. All of the molecules under investigation have been found to conform to Lipinski's rule of five and the Ghose rule, indicating their potential for oral bioavailability.

In particular, the relationship between the TPSA value and the permeability of the blood-brain barrier has been considered, with TPSA below 90 Å^2 being associated with higher permeability and those above 140 Å^2 being linked to lower permeability (Hitchcock & Pennington, 2006; Pajouhesh & Lenz, 2005). Among the test compounds, cycloartomunoxanthone exhibits the lowest TPSA of 96.36 Å^2, while dihydrocycloartomunin and cycloartobiloxanthone shows the highest TPSA, that is 109.36 Å^2. However, artomunoxanthentrione and cycloartomunin showed TPSA values of 103.04 Å^2 and 98.36 Å^2, respectively. Normatrelvir, the standard inhibitor exhibits a TPSA of 131.40 Å^2.

According to Lipinski's rule of five, drugs intended for oral administration should have a lipophilicity value below 5.0. All molecules investigated in this study were found to have lipophilicity (MLogP) below this threshold. Artomunoxanthentrione exhibited the lowest MLogP value as a test compound, which is 1.06, whereas that of cycloartomunoxanthone is 1.84 (highest among the test compounds). Cycloartomunin, dihydrocycloartomunin, and cycloartobiloxanthone have MLogP values of 1.77, 1.77, and 1.63, respectively (as shown in Table 2). The

standard inhibitor, nirmatrelvir, has a value of 0.41. Water solubility (LogS (ESOL)) was also investigated for each compound. Cycloartomunin, dihydrocycloartomunin, cycloartobiloxanthone, artomunoxanthentrione, and cycloartomunoxanthone have LogS (ESOL) values of −6.10, −6.39, −5.46, −6.05, and −5.67, respectively. Nirmatrelvir occupies a LogS (ESOL) of −3.58. All five of the test compounds were found to have poor water solubility except cycloartobiloxanthone and cycloartomunoxanthone (both are moderately soluble). However, all the test compounds and the standard inhibitor show high gastrointestinal absorption, and each has a bioavailability score of 0.55, except artomunoxanthentrione (0.56). Cycloartobiloxanthone and Cycloartomunoxanthone were found to be substrates of the P-glycoprotein (P-gp).

In terms of toxicity, the lethal dose 50 (LD50) for cycloartomunin, dihydrocycloartomunin, cycloartobiloxanthone, artomunoxanthentrione, and cycloartomunoxanthone are 5000, 5000, 2500, 120, and 5000 mg/kg, respectively. All test compounds except artomunoxanthentrione belong to toxicity class 5. The toxicity class of artomunoxanthentrione is 3. Nirmatrelvir, on the other hand, has a LD50 of 3000 mg/kg and belongs to toxicity class 5. It is important to mention that the higher the toxicity class, the safer the molecule would be while considering the amount administered. The bioavailability radars of the molecules are shown in Figure 3. The computer-generated estimates of the phytochemicals' hepatotoxicity, carcinogenicity, immunotoxicity, mutagenicity, and cytotoxicity profiles have been meticulously recorded (Table 2). The toxicity data affirms that the most of the compounds, as indicated in green and light green, are safe in terms of their hepatotoxic, carcinogenic, mutagenic and cytotoxic profiles. Nonetheless, certain immunotoxicity concerns are indicated in red. The selected drug, Nirmatrelvir, is safe according to all of the toxicity profiles and is indicated in green and light green. A higher number of greens indicate more safety in terms of toxicity.
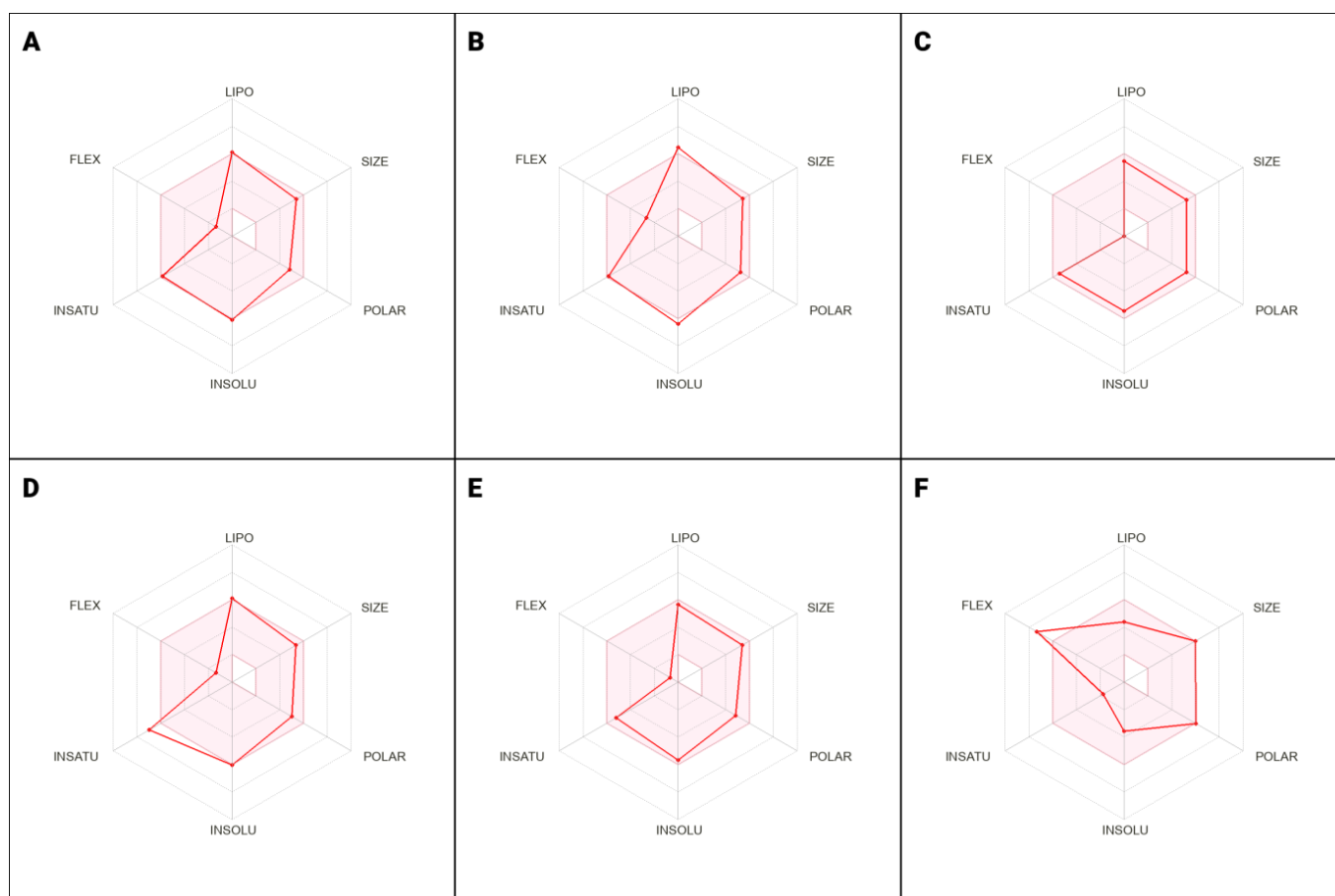
Figure 3: The bioavailability radars of (A) cycloartomunin, (B) dihydrocycloartomunin, (C) cycloartobiloxanthone, (D) artomunoxanthentrione, (E) cycloartomunoxanthone, and (F) nirmatrelvir retrieved from SwissADME. The colored zone is the suitable physicochemical space for oral bioavailability. LIPO (Lipophilicity): −0.7 < XLOGP3 < +5.0; SIZE: 150g/mol < MV < 500g/mol; POLAR (Polarity): 20Å² < TPSA < 130Å²; INSOLU (Insolubility): −6 < Log S (ESOL) < 0; INSATU (Insaturation): 0.25 < Fraction Csp3 < 1; FLEX (Flexibility): 0 < Num. rotatable bonds < 9.

Table 2: The physicochemical, pharmacokinetic, and pharmacodynamic properties of the molecules with the top 6 docking scores retrieved from SwissADME and Protox-II.

Property	Cycloarto munin	Dihydrocycloa rtomunin	Cycloartobilo xanthone	Artomunoxan thentrione	Cycloartomu noxanthone	Nirmatrelvir (standard)
MW (g/mol)	448.46	450.48	434.44	444.43	448.46	499.53
TPSA (Å²)	98.36	109.36	109.36	103.04	96.36	131.40
MLogP	1.77	1.77	1.63	1.06	1.84	0.41
LogS (ESOL)	−6.10	−6.39	−5.46	−6.05	−5.67	−3.58
ESOL Class	Poorly soluble	Poorly soluble	Moderately soluble	Poorly soluble	Moderately soluble	Soluble
GI absorption	High	High	High	High	High	High
Bioavailability score	0.55	0.55	0.55	0.56	0.55	0.55
BBB permeant	No	No	No	No	No	No
P-gp substrate	No	No	Yes	No	Yes	Yes
Lipinski's RO5 vio.	0	0	0	0	0	0
Ghose filter vio.	0	0	0	0	0	0
LD50 (mg/kg)	5000	5000	2500	120	5000	3000
Toxicity class	5	5	5	3	5	5
Hepatotoxicity	🟢	🟢	🟢	🟢	🟢	🟢
Carcinogenicity	🟢	🟢	🟢	🟢	🟢	🟢
Immunotoxicity	🔴	🔴	🔴	🔴	🔴	🟢
Mutagenicity	🟢	🟢	🟢	🟢	🟢	🟢
Cytotoxicity	🟢	🟢	🟢	🟢	🟢	🟢

MW: molecular weight; TPSA: topological polar surface area; MLogP: lipophilicity; LogS (ESOL): water solubility; ESOL class: water solubility class; GI absorption: gastrointestinal absorption; bioavailability score: Abbott bioavailability score; BBB permeant: blood-brain barrier permeability; P-gp substrate: interaction with P-glycoprotein; Lipinski Vio: number of violations of Lipinski's rule of Gve; Ghose Vio: number of violations of Ghose's rule; LD50 (mg/kg):lethal dose 50; toxicity class: class based on LD50 value, various colors primarily indicated the toxicity profiles of each chemical; green denoted safety or non-toxicity, light green signified a moderate level of safety, red indicated harm or toxicity.

Conclusion

The goal of this study was to look at compelling compounds from breadfruit (*Artocarpus altilis)* in order to trace possible inhibitors of the M^{pro} enzyme of SARS-CoV-2. Artomunoxanthentrione and cycloartomunoxanthone were found to have affinities above and equal to the standard inhibitor. Artomunoxanthentrione had the highest binding affinity when docked with the target. Moreover, cycloartomunin, dihydrocycloartomunin, and cycloartobiloxanthone also displayed good interactions with the target. This study, however, solely investigates the *in-silico* characteristics and profiles of the phytochemicals from *Artocarpus altilis*. Additional validations are demanded to confirm the efficacy and potentiality of the test compounds as potential inhibitors of the SARS-CoV-2 target enzyme. As a result of this, our study findings suggest cycloartomunin, dihydrocycloartomunin, cycloartobiloxanthone, artomunoxanthentrione, and cycloartomunoxanthone as promising candidates against the M^{pro} enzyme of SARS-CoV-2.

Conflicts of Interest

The authors declare no conflicts of interest.

Supplement
Figures: Go to the following link to download high resolutions of the figures:
https://drive.google.com/drive/folders/1qZN5BscDg2d fCHeBAWseGvOnv0FQsWYG?usp=sharing

References

Ajiboye, B. O., Ojo, O. A., Oyinloye, B. E., Okesola, M. A., Oluwatosin, A., Boligon, A. A., & Kappo, A. P. (2020). Investigation of the In Vitro Antioxidant Potential Of Polyphenolic-Rich Extract of *Artocarpus heterophyllus* Lam Stem Bark and Its Antidiabetic Activity In Streptozotocin-Induced Diabetic Rats. *Journal of Evidence-Based Integrative Medicine*, *25*, 2515690X2091612. https://doi.org/10.1177/251569 0X20916123.

Banerjee, P., Eckert, A. O., Schrey, A. K., & Preissner, R. (2018). ProTox-II: A webserver for the prediction of toxicity of chemicals. *Nucleic Acids Research*, *46*(W1), Article W1. https://doi.org/10.1093/nar/gky318.

Baroroh, S.Si., M.Biotek., U., Muscifa, Z. S., Destiarani, W., Rohmatullah, F. G., & Yusuf, M. (2023). Molecular interaction analysis and visualization of protein-ligand docking using Biovia Discovery Studio Visualizer. *Indonesian Journal of Computational Biology (IJCB)*, *2*(1), 22. https://doi.org/10.24198/ijcb.v2i1.46322.

BIOVIA, Dassault Systèmes, [Discovery Studio Visualizer], [v21.1.0.20298], San Diego: Dassault Systèmes, [2020]. https://discover.3ds.com/discovery-studio-visualizer-download.

Citarella, A., Scala, A., Piperno, A., & Micale, N. (2021). SARS-CoV-2 Mpro: A Potential Target for Peptidomimetics and Small-Molecule Inhibitors. *Biomolecules*, *11*(4), 607. https://doi.org/10.3390/biom11040607.

Daina, A., Michielin, O., & Zoete, V. (2017). SwissADME: A free web tool to evaluate pharmacokinetics, drug-likeness and medicinal chemistry friendliness of small molecules. *Scientific Reports*, *7*(1), Article 1. https://doi.org/10.1038/srep42717.

Dejnirattisai, W., Huo, J., Zhou, D., Zahradník, J., Supasa, P., Liu, C., Duyvesteyn, H. M. E., Ginn, H. M., Mentzer, A. J., Tuekprakhon, A., Nutalai, R., Wang, B., Dijokaite, A., Khan, S., Avinoam, O., Bahar, M., Skelly, D., Adele, S., Johnson, S. A., … Young, P. (2022). SARS-CoV-2 Omicron-B.1.1.529 leads to widespread escape from neutralizing antibody responses. *Cell*, *185*(3), Article 3. https://doi.org/10.1016/ j.cell.2021.12. 046.

Deng, Q., Rasool, R. ur, Russell, R. M., Natesan, R., & Asangani, I. A. (2021). Targeting androgen regulation of TMPRSS2 and ACE2 as a therapeutic strategy to combat COVID-19. *IScience*, *24*(3), Article 3. https://doi.org/10.1016/ j.isci.2021.102254.

Dharmashekara, C., Pradeep, S., Prasad, S. K., Jain, A. S., Syed, A., Prasad, K. S., Patil, S. S., Beelagi, M. S., Srinivasa, C., & Shivamallu, C. (2021). Virtual screening of potential phyto-candidates as therapeutic leads against SARS-CoV-2 infection. *Environmental Challenges*, *4*, 100136. https://doi.org/10.1016/j.envc.2021.100136.

Du, X., Li, Y., Xia, Y.-L., Ai, S.-M., Liang, J., Sang, P., Ji, X.-L., & Liu, S.-Q. (2016). Insights into Protein–Ligand Interactions: Mechanisms, Models, and Methods. *International Journal of Molecular Sciences*, *17*(2), 144. https://doi.org/10.3390/ijms17020144.

Guedes, I. A., De Magalhães, C. S., & Dardenne, L. E. (2014). Receptor–ligand molecular docking. *Biophysical Reviews*, *6*(1), 75–87. https://doi.org/10.1007/s12551-013-0130-2.

Guex, N., & Peitsch, M. C. (1997). SWISS-MODEL and the Swiss-Pdb Viewer: An environment for

comparative protein modeling. *Electrophoresis*, *18*(15), Article 15. https://doi.org/10.1002/elps.1150181505.

Gui, H., Zhang, Z., Chen, B., Chen, Y., Wang, Y., Long, Z., Zhu, C., Wang, Y., Cao, Z., & Xie, Q. (2023). Development and validation of a nomogram to predict failure of 14-day negative nucleic acid conversion in adults with non-severe COVID-19 during the Omicron surge: A retrospective multicenter study. *Infectious Diseases of Poverty*, *12*(1), 7. https://doi.org/10.1186/s40249-023-01057-4.

Hitchcock, S. A., & Pennington, L. D. (2006). Structure−Brain Exposure Relationships. *Journal of Medicinal Chemistry*, *49*(26), Article 26. https://doi.org/10.1021/jm060642i.

Hu, B., Guo, H., Zhou, P., & Shi, Z.-L. (2021). Characteristics of SARS-CoV-2 and COVID-19. *Nature Reviews Microbiology*, *19*(3), Article 3. https://doi.org/10.1038/s41579-020-00459-7.

Hu, Q., Xiong, Y., Zhu, G., Zhang, Y., Zhang, Y., Huang, P., & Ge, G. (2022). The SARS-CoV-2 main protease (M ^{pro}): Structure, function, and emerging therapies for COVID-19. *MedComm*, *3*(3), e151. https://doi.org/10.1002/mco2.151.

Huang, J., Yin, D., Qin, X., Yu, M., Jiang, B., Chen, J., Cao, Q., & Tang, Z. (2022). Case report: Application of nirmatrelvir/ritonavir to treat COVID-19 in a severe aplastic anemia child after allogeneic hematopoietic stem cell transplantation. *Frontiers in Pediatrics*, *10*, 935118. https://doi.org/10.3389/fped.2022.935118.

Huynh, T., Cornell, W., & Luan, B. (2021). In silico Exploration of Inhibitors for SARS-CoV-2's Papain-Like Protease. *Frontiers in Chemistry*, *8*, 624163.https://doi.org/10.3389/fchem.2020.624163.

Inoue, H., & Todo, Y. (2020). The propagation of economic impacts through supply chains: The case of a mega-city lockdown to prevent the spread of COVID-19. *PLOS ONE*, *15*(9), Article 9. https://doi.org/10.1371/journal.pone.0239251.

Jalal, T. K., Ahmed, I. A., Mikail, M., Momand, L., Draman, S., Isa, M. L. M., Abdull Rasad, M. S. B., Nor Omar, M., Ibrahim, M., & Abdul Wahab, R. (2015). Evaluation of Antioxidant, Total Phenol and Flavonoid Content and Antimicrobial Activities of Artocarpus altilis (Breadfruit) of Underutilized Tropical Fruit Extracts. *Applied Biochemistry and Biotechnology*, *175*(7), 3231–3243. https://doi.org/10.1007/s12010-015-1499-0.

Khan, T., Lawrence, A. J., Azad, I., Raza, S., Joshi, S., & Khan, A. R. (2019). Computational Drug Designing and Prediction Of Important Parameters Using in silico Methods- A Review. *Current Computer-Aided Drug Design*, *15*(5), 384–397. https://doi.org/10.2174/157339981566619032612 0006.

Kim, S., Chen, J., Cheng, T., Gindulyte, A., He, J., He, S., Li, Q., Shoemaker, B. A., Thiessen, P. A., Yu, B., Zaslavsky, L., Zhang, J., & Bolton, E. E. (2019). PubChem 2019 update: Improved access to chemical data. *Nucleic Acids Research*, *47*(D1), D1102–D1109. https://doi.org/10.1093/nar/gky1033

Kim, S., Thiessen, P. A., Bolton, E. E., Chen, J., Fu, G., Gindulyte, A., Han, L., He, J., He, S., Shoemaker, B. A., Wang, J., Yu, B., Zhang, J., & Bryant, S. H. (2016). PubChem Substance and Compound databases. *Nucleic Acids Research*, *44*(D1), D1202–D1213. https://doi.org/10.1093/nar/gkv951.

Li, Q., Wu, J., Nie, J., Zhang, L., Hao, H., Liu, S., Zhao, C., Zhang, Q., Liu, H., Nie, L., Qin, H., Wang, M., Lu, Q., Li, X., Sun, Q., Liu, J., Zhang, L., Li, X., Huang, W., & Wang, Y. (2020). The Impact of Mutations in SARS-CoV-2 Spike on Viral Infectivity and Antigenicity. *Cell*, *182*(5), Article 5. https://doi.org/10.1016/ j.cell.2020. 07. 012.

Li, X., Lidsky, P. V., Xiao, Y., Wu, C.-T., Garcia-Knight, M., Yang, J., Nakayama, T., Nayak, J. V., Jackson, P. K., Andino, R., & Shu, X. (2021). Ethacridine inhibits SARS-CoV-2 by inactivating viral particles. *PLOS Pathogens*, *17*(9), Article 9. https://doi.org/10.1371/journal.ppat.1009898.

Lill, M. A., & Danielson, M. L. (2011). Computer-aided drug design platform using PyMOL. *Journal of Computer-Aided Molecular Design*, *25*(1), Article 1. https://doi.org/10.1007/s10822-010-9395-8.

Lipinski, C. A., Lombardo, F., Dominy, B. W., & Feeney, P. J. (2001). Experimental and computational approaches to estimate solubility and permeability in drug discovery and development settings 1PII of original article: S0169-409X(96)00423-1. The article was originally published in Advanced Drug Delivery Reviews 23 (1997) 3–25. 1. *Advanced Drug Delivery Reviews*, *46*(1–3), Article 1–3. https://doi.org/10.1016/S0169-409X(00)00129-0.

Liu, Y., Yang, X., Gan, J., Chen, S., Xiao, Z.-X., & Cao, Y. (2022). CB-Dock2: Improved protein–ligand blind docking by integrating cavity detection, docking and homologous template fitting. *Nucleic Acids Research*, *50*(W1), Article W1. https://doi.org/10.1093/nar/gkac394.

Ludwig, S., & Zarbock, A. (2020). Coronaviruses and SARS-CoV-2: A Brief Overview. *Anesthesia & Analgesia*, *131*(1), 93–96. https://doi.org/10.1213/ANE.0000000000004845.

Maycock, A. L., Abeles, R. H., Salach, J. I., & Singer, T. P. (1976). The structure of the covalent adduct formed by the interaction of 3-dimethylamino-1-propyne and the flavine of mitochondrial amine oxidase. *Biochemistry*, *15*(1), Article 1. https://doi.org/10.1021/bi00646a018.

Miyah, Y., Benjelloun, M., Lairini, S., & Lahrichi, A. (2022). COVID-19 Impact on Public Health, Environment, Human Psychology, Global Socioeconomy, and Education. *The Scientific World Journal*, *2022*, 1–8. https://doi.org/10.1155/2022/5578284.

Morris, G. M., & Lim-Wilby, M. (2008). Molecular Docking. In A. Kukol (Ed.), *Molecular Modeling of Proteins* (Vol. 443, pp. 365–382). Humana Press. https://doi.org/10.1007/978-1-59745-177-2_19.

Nogara, P. A., Saraiva, R. D. A., Caeran Bueno, D., Lissner, L. J., Lenz Dalla Corte, C., Braga, M. M., Rosemberg, D. B., & Rocha, J. B. T. (2015). Virtual Screening of Acetylcholinesterase Inhibitors Using the Lipinski's Rule of Five and ZINC Databank. *BioMed Research International*, *2015*, 1–8. https://doi.org/10.1155/2015/870389.

Pajouhesh, H., & Lenz, G. R. (2005). Medicinal chemical properties of successful central nervous system drugs. *NeuroRX*, *2*(4), Article 4. https://doi.org/10.1602/neurorx.2.4.541.

Pantsar, T., & Poso, A. (2018). Binding Affinity via Docking: Fact and Fiction. *Molecules*, *23*(8), 1899. https://doi.org/10.3390/molecules23081899.

Park, J. J., Lee, J., Seo, Y. B., & Na, S. H. (2022). Nirmatrelvir/Ritonavir Prescription Rate and Outcomes in Coronavirus Disease 2019: A Single Center Study. *Infection & Chemotherapy*, *54*(4), 757. https://doi.org/10.3947/ic.2022.0123.

Patnaik, U. J. 2. (2021). Review article on COVID-19 and Guillain-Barré syndrome. *Frontiers in Bioscience-Scholar*, *13*(1), Article 1. https://doi.org/10.52586/S555.

Riasari, H., Nurlalela, S., & Gumilang, G. C. (2019). Anti-Inflammatory Activity of Artocarpus altilis (Parkinson) Fosberg in Wistar Male Rats. *Pharmacology and Clinical Pharmacy Research*, *4*(1), 22. https://doi.org/10.15416/pcpr.v4i1.21397.

Rodrigues, L., Bento Cunha, R., Vassilevskaia, T., Viveiros, M., & Cunha, C. (2022). Drug Repurposing for COVID-19: A Review and a Novel Strategy to Identify New Targets and Potential Drug Candidates. *Molecules*, *27*(9), 2723. https://doi.org/10.3390/molecules27092723.

Rose, P. W., Prlić, A., Altunkaya, A., Bi, C., Bradley, A. R., Christie, C. H., Costanzo, L. D., Duarte, J. M., Dutta, S., Feng, Z., Green, R. K., Goodsell, D. S., Hudson, B., Kalro, T., Lowe, R., Peisach, E., Randle, C., Rose, A. S., Shao, C., … Burley, S. K. (2017). The RCSB protein data bank: Integrative view of protein, gene and 3D structural information. *Nucleic Acids Research*, *45*(D1), D271–D281. https://doi.org/10.1093/nar/gkw1000.

Sikarwar, M. S., Hui, B. J., Subramaniam, K., Valeisamy, B. D., Yean, L. K., & Balaji, K. (2014). A Review on *Artocarpus altilis* (Parkinson) Fosberg (breadfruit). *Journal of Applied Pharmaceutical Science*, *4*(8), 091–097. https://doi.org/10.7324/JAPS.2014.40818.

Sousa, S. F., Fernandes, P. A., & Ramos, M. J. (2006). Protein–ligand docking: Current status and future challenges. *Proteins: Structure, Function, and Bioinformatics*, *65*(1), 15–26. https://doi.org/10.1002/prot.21082.

Tara Kamal,. (2012). Investigation of antioxidant activity and phytochemical constituents of Artocarpus altilis. *Journal of Medicinal Plants Research*, *6*(26). https://doi.org/10.5897/JMPR12.666.

Turi, C. E., Liu, Y., Ragone, D., & Murch, S. J. (2015). Breadfruit (Artocarpus altilis and hybrids): A traditional crop with the potential to prevent hunger and mitigate diabetes in Oceania. *Trends in Food Science & Technology*, *45*(2), 264–272. https://doi.org/10.1016/j.tifs.2015.07.014.

Vivek-Ananth, R. P., Mohanraj, K., Sahoo, A. K., & Samal, A. (2023). IMPPAT 2.0: An Enhanced and Expanded Phytochemical Atlas of Indian Medicinal Plants. *ACS Omega*, *8*(9), 8827–8845. https://doi.org/10.1021/acsomega.3c00156.

Yu, W., & MacKerell, A. D. (2017). Computer-Aided Drug Design Methods. In P. Sass (Ed.), *Antibiotics* (Vol. 1520, pp. 85–106). Springer New York. https://doi.org/10.1007/978-1-4939-6634-9_5.

Zhong, L., Diagne, M., Wang, W., & Gao, J. (2021). Country distancing increase reveals the effectiveness of travel restrictions in stopping COVID-19 transmission. *Communications Physics*, *4*(1), Article 1. https://doi.org/10.1038/s42005-021-00620-5.